

Article

An Overview of Strengths and Directionalities of Noncovalent Interactions: σ -Holes and π -Holes

Peter Politzer * and Jane S. Murray

Department of Chemistry, University of New Orleans, New Orleans, LA 70148, USA; jane.s.murray@gmail.com

* Correspondence: ppolitze@uno.edu

Received: 12 March 2019; Accepted: 16 March 2019; Published: 21 March 2019



Abstract: Quantum mechanics, through the Hellmann–Feynman theorem and the Schrödinger equation, show that noncovalent interactions are classically Coulombic in nature, which includes polarization as well as electrostatics. In the great majority of these interactions, the positive electrostatic potentials result from regions of low electronic density. These regions are of two types, designated as σ -holes and π -holes. They differ in directionality; in general, σ -holes are along the extensions of covalent bonds to atoms (or occasionally between such extensions), while π -holes are perpendicular to planar portions of molecules. The magnitudes and locations of the most positive electrostatic potentials associated with σ -holes and π -holes are often approximate guides to the strengths and directions of interactions with negative sites but should be used cautiously for this purpose since polarization is not being taken into account. Since these maximum positive potentials may not be in the immediate proximities of atoms, interatomic close contacts are not always reliable indicators of noncovalent interactions. This is demonstrated for some heterocyclic rings and cyclic polyketones. We briefly mention some problems associated with using Periodic Table Groups to label interactions resulting from σ -holes and π -holes; for example, the labels do not distinguish between these two possibilities with differing directionalities.

Keywords: noncovalent interactions; electrostatic potentials; σ -holes; π -holes; directionalities; close contacts; electrostatics; polarization

1. σ -Holes and π -Holes

The explosion of interest in halogen bonding and its various analogues in recent years seems to have borne out Schneider’s observation in 2009 that “the chemistry of the last century was largely the chemistry of covalent bonding, whereas that of the present century is more likely to be the chemistry of noncovalent bonding” [1]. While this statement overlooks the fact that neither covalent nor noncovalent bonding is uniquely defined, nor is there a clear-cut distinction between them, Schneider’s point is basically well taken.

Most noncovalent bonding (including hydrogen bonds) can be explained in terms of σ -holes and π -holes [2–5]. A σ -hole is a region of lower electronic density on the outer side of a covalently-bonded atom, on the extension of the bond. A π -hole is also a region of lower electronic density, but it is above and below a planar portion of a molecule. These regions of lower electronic density, which reflect the anisotropies of covalently-bonded atoms [6–11], often (but not always) give rise to positive electrostatic potentials. Through these positive potentials, the molecule can interact attractively with negative sites, such as lone pairs, π -electrons, and anions [2–5]. This accounts for numerous noncovalent interactions that have been known for many years [3,4,11–18], and provides important routes to self-assembly in crystal engineering [19,20].

The terms σ -hole and π -hole are useful umbrellas, each encompassing a large group of interactions that are fundamentally similar although involving different Groups of the Periodic Table. The

distinction between the two groups is directionality. Interactions resulting from σ -holes are usually approximately linear and along the extensions of the bonds that gave rise to the σ -holes. (There are some exceptions, as will be discussed, because of overlapping of positive potentials). Interactions due to π -holes are approximately perpendicular to the planar molecular regions that produced the π -holes. Note that hydrogen bonding fits into the σ -hole category [11,21]; it is analogous to monovalent halogen interactions [22].

There is now an increasing tendency to go beyond σ -hole and π -hole in classifying noncovalent interactions and to use a different label for each Group of the Periodic Table [20,23]: halogen bonding for Group VII, chalcogen bonding for Group VI, pnictogen bonding for Group V, tetrel bonding for Group IV, and triel bonding for Group III. These labels are now quite widely used. They do identify the Group, but they do not reveal the unifying similarity of all of the interactions due to σ -holes and that of all those due to π -holes.

The Group labels also introduce ambiguities. For example, many covalently-bonded atoms can have both σ -holes and π -holes. Simply identifying the Group does not distinguish between them. Calling an interaction a tetrel bond, for instance, does not indicate whether it arises from a σ -hole or a π -hole—an important distinction from the standpoint of directionality.

2. Molecular Electrostatic Potentials

Since molecular electrostatic potentials have played an important part in elucidating the natures of interactions due to σ -holes and π -holes, we will briefly review this property. Consider a point charge Q_1 located at \mathbf{R}_1 . It creates an electrostatic potential in the surrounding space, the value of which at a location \mathbf{r} is $Q_1/|\mathbf{r} - \mathbf{R}_1|$. The significance of this potential means that if a second point charge Q_2 is brought to the point \mathbf{r} , then the interaction energy between the two charges will be $\Delta E = Q_1 Q_2 / |\mathbf{r} - \mathbf{R}_1|$. If the two charges have the same sign, then $\Delta E > 0$ and the interaction is unfavorable; if the signs are different, then $\Delta E < 0$ and the interaction is favorable (attractive).

A molecule can be regarded as a collection of point charges, the nuclei, and the electrons. The electrostatic potential $V(\mathbf{r})$ that the molecule produces at any point \mathbf{r} is simply the sum of their individual contributions. Since the positions of the electrons cannot be specified, this requires integrating over the molecule's average electronic density $\rho(\mathbf{r})$. $V(\mathbf{r})$ is given rigorously by Equation (1), in which Z_A is the charge on nucleus A, located at \mathbf{R}_A :

$$V(\mathbf{r}) = \sum_A \frac{Z_A}{|\mathbf{R}_A - \mathbf{r}|} - \int \frac{\rho(\mathbf{r}') d\mathbf{r}'}{|\mathbf{r}' - \mathbf{r}|} \quad (1)$$

The electrostatic potential is a real physical property, an observable, which can be determined either experimentally by diffraction techniques [24–26] or computationally. (In contrast, atomic charges, which are so widely used, are arbitrarily defined and have no physical basis [27,28]). The electrostatic potential indicates how specific regions of a molecule will interact with external charges; e.g., regions in which $V(\mathbf{r})$ is positive (negative) will interact favorably (unfavorably) with negative sites. In the context of noncovalent interactions, $V(\mathbf{r})$ is now typically computed on the molecular surface defined, following Bader et al [29], by the 0.001 au contour of the electronic density. The potential on this surface is designated as $V_S(\mathbf{r})$ and its most positive and negative values (of which there may be several) as $V_{S,\max}$ and $V_{S,\min}$.

It must be stressed that, as shown in Equation (1), the molecular electrostatic potential reflects the positive contributions of the nuclei as well as the negative ones of the electrons. The assumption is sometimes made that “electron-rich” regions will have negative $V(\mathbf{r})$ and “electron-poor” ones will have positive $V(\mathbf{r})$. This is not necessarily the case; the electrostatic potential does not simply follow the electronic density [30–34]. The nuclei must be taken into account. This is illustrated by the nitrogen molecule, N_2 . There is a considerable buildup of electronic density (formally a triple bond) in its internuclear region [35], yet Figure 1 shows that $V(\mathbf{r})$ is positive there. This is due to the two +7

nuclei. $V(\mathbf{r})$ is negative in the lone pair regions, in which the effect of just one nucleus is primarily felt. (Electrostatic potentials presented in this work are on the 0.001 au molecular surfaces and are computed at the density functional M06-2X/6-31G(d,p) level, using Gaussian 09 [36] and the Wave Function Analysis - Surface Analysis Suite (WFA-SAS) code [37].)

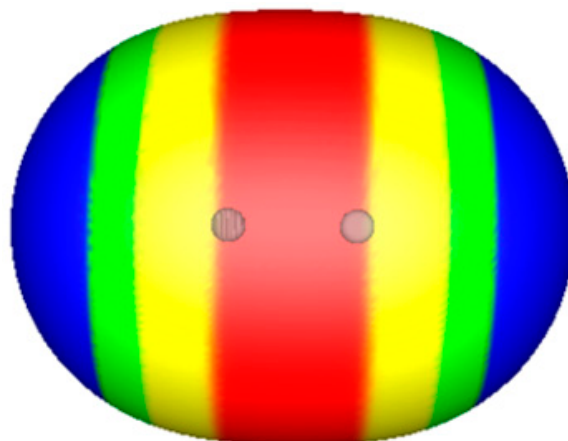


Figure 1. Computed electrostatic potential on 0.001 au molecular surface of N_2 . Gray circles indicate positions of nuclei. Color ranges in kcal/mol: red, more positive than 6; yellow, between 6 and 3; green, between 3 and 0; blue, negative.

3. Coulombic Nature of Interactions

The preceding discussion has emphasized the Coulombic nature of interactions arising from σ -holes and π -holes. This is in full accord with the quantum-mechanical Hellmann–Feynman theorem, which shows rigorously that the forces felt by the nuclei in a molecule or complex are purely classically Coulombic [38,39].

This should not really be surprising. As has been pointed out [40,41], the only attractive terms in the Hamiltonian are Coulombic. Lennard-Jones and Pople summarized the situation [42]: “There is only one source of attraction between two atoms, and that is the force between electrons and nuclei. But there are three counteracting influences: the nuclei repel each other, the electrons repel each other, and the kinetic energy of the electrons increases when a chemical bond is formed.” The forces are entirely Coulombic.

This explanation of the interactions may appear oversimplified to those accustomed to thinking in terms of exchange, Pauli repulsion, etc., but these terms refer to mathematical requirements that a wave function must satisfy: indistinguishability of electrons and antisymmetry. They do not correspond to physical forces, as discussed in greater detail elsewhere [43–45]. As Levine put it [46], “there are no ‘mysterious quantum-mechanical forces’ acting in molecules”.

There is an important caveat that must be part of the Coulombic explanation of intermolecular interactions. They cannot be fully described in terms of the unperturbed charge distributions of the two molecules in their ground states. This would be physically unrealistic because it ignores the polarization of each molecule’s charge distribution by the electric field of the other, which affects the Coulombic interactions between them [43,47–49]. The effects of polarization are often relatively minor, but they can also be quite significant. For instance, the most positive electrostatic potential associated with the chlorine σ -hole in H_3C-Cl is near zero, yet it can form the $H_3C-Cl-O=CH_2$ complex [50] because the electric field of the negative oxygen of $O=CH_2$ induces a significant positive potential on the chlorine.

Halogen bonding and other interactions related to σ -holes have frequently been described as “donor-acceptor”, invoking the valence-bond charge-transfer model of Mulliken [51] (later put in molecular orbital terms by Flurry [52]). As was already pointed out some time ago however, Mulliken’s charge transfer formalism pertains to the transition of a ground-state noncovalent complex to a

low-lying excited state [53,54]. It was not intended to elucidate the bonding in the ground-state complex and does not provide a physical basis for it.

It is now increasingly recognized that charge transfer in noncovalent interactions is simply a mathematical modeling of the actual physical phenomenon, which is polarization [40,55–59]. Note in particular the recent analysis by Brinck and Borrforss [60], who give a “red card” to charge transfer. (They are obviously soccer enthusiasts).

The shifts in bond stretching frequencies that are often used to support a charge transfer interpretation can readily be explained and predicted in terms of the electric fields of the negative sites and the permanent and induced dipole moments of the molecules bearing the σ -holes [61,62]. Charge transfer is not invoked.

4. Significance of $V_{S,max}$

Equation (1) shows that the electrostatic potential at any point r reflects contributions from all of the nuclei and electrons of the molecule, especially those of neighboring atoms in close proximity. These can influence both the magnitude and the location of the positive potential arising from a σ -hole or π -hole. For instance, the locally most positive molecular surface value ($V_{S,max}$) due to a σ -hole may deviate somewhat from the extension of the bond with which the σ -hole is associated [5].

In Figure 2 is the electrostatic potential on the 0.001 au molecular surface of $P(CH_3)Cl_2$. The phosphorus has positive regions corresponding to σ -holes produced by the H_3C-P and the two $Cl-P$ bonds. Each of these regions has a $V_{S,max}$; their magnitudes are 10, 28, and 28 kcal/mol. However, these $V_{S,max}$ are not directly on the extensions of the bonds; they deviate by about 15° (away from the phosphorus lone pair), reflecting the asymmetrical influence of nearby atoms.

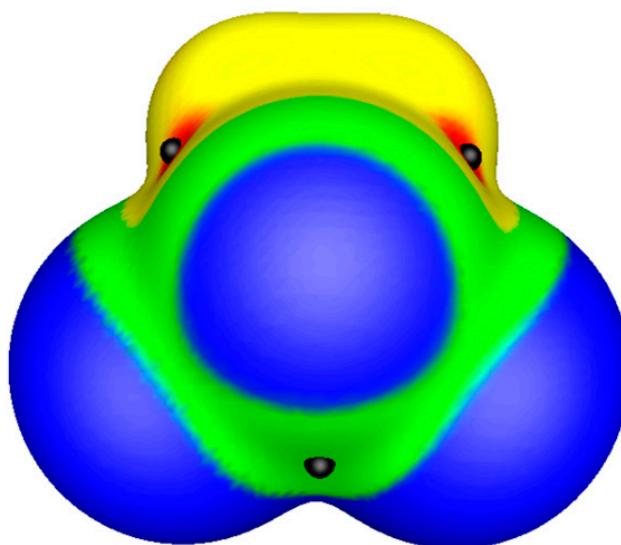


Figure 2. Computed electrostatic potential on 0.001 au molecular surface of $P(CH_3)Cl_2$. The phosphorus is in the center foreground, the chlorines are in the lower left and lower right. Black hemispheres indicate $V_{S,max}$ on the phosphorus, corresponding to the σ -holes due to the H_3C-P and the two $Cl-P$ bonds. Color ranges, in kcal/mol: red, more positive than 26; yellow, between 26 and 13; green, between 13 and 0; blue, negative.

Such deviations are quite common for Group VI and Group V atoms [5], which are frequently in asymmetrical molecular frameworks. For Groups VII and IV, on the other hand, the $V_{S,max}$ due to σ -holes tend to be close to the extensions of the bonds. This is because Group VII atoms protrude from the molecular framework and do not have near neighbors, while for Group IV, there are neighbors on all sides, even if they are not the same.

As Figure 2 shows, covalently-bonded Group V atoms, like those in Groups VI and VII, often have regions of negative potential on their surfaces, as well as positive ones reflecting σ -holes [3,5,11]. These negative regions can interact attractively with positive sites; this has indeed been observed in crystallographic surveys of halide [16], sulfide [17], and selenide [63] crystal structures.

Note in Figure 2 that the chlorines in $\text{P}(\text{CH}_3)\text{Cl}_2$ do not have positive potentials on the extensions of the P–Cl bonds, although they do have σ -holes there. The presence of σ -holes (lower electronic densities) is confirmed by the distance from each chlorine nucleus to the 0.001 au contour along the bond extension being less (1.99 Å) than that perpendicular to the bond (2.12 Å). However, the σ -holes do not result in positive electrostatic potentials. Such situations are particularly common for first row atoms due to their high electronegativities and low polarizabilities [3,11]. On the other hand, if these atoms are put into sufficiently strongly electron-withdrawing molecular environments, e.g., the fluorine in FCN, then their σ -holes can also give rise to positive electrostatic potentials [64–66].

Phosphorus can have π -holes as well as σ -holes. Figure 3 shows the electrostatic potential above and below the planar $\text{P}(\text{Cl})\text{O}_2$ molecule. There are $V_{S,\text{max}}$ of 53 kcal/mol essentially above and below the phosphorus nucleus, reflecting the lower electronic densities of π -holes. There is also a $V_{S,\text{max}}$ of 21 kcal/mol on the chlorine, on the extension of the P–Cl bond, due to a σ -hole.

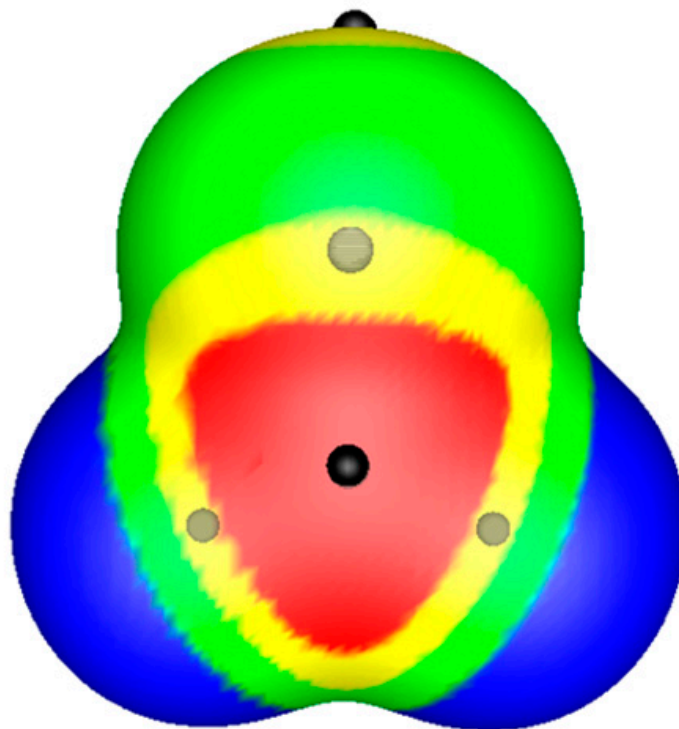


Figure 3. Computed electrostatic potential on 0.001 au molecular surface of $\text{P}(\text{Cl})\text{O}_2$, which is planar. The phosphorus is at the center, the chlorine is at the top. Gray circles indicate positions of nuclei. Black hemispheres show locations of $V_{S,\text{max}}$; there is one directly above and below the phosphorus nucleus, due to a π -hole, and one on the chlorine, corresponding to a σ -hole on the extension of the P–Cl bond. Color ranges, in kcal/mol: red, more positive than 26; yellow, between 26 and 13; green, between 13 and 0; blue, negative.

What is the significance of the $V_{S,\text{max}}$ on the 0.001 au surface of a molecule? Are they guides to the interactions of the molecule with negative sites?

In principle, these questions need to be approached cautiously. First it must be recognized that these $V_{S,\text{max}}$ are local maxima only on the particular contour of the electronic density; in the present case, this is the 0.001 au. They are not global maxima; it has been proven that the only positive sites in

a molecule, from a global standpoint, are the nuclei [67]. Accordingly, the $V_{S,max}$ are not positive sites in a global sense.

In addition, an approaching negative site will interact not only with the $V_{S,max}$ but with at least the entire positive region and perhaps beyond. Furthermore, as already pointed out, the electric field of the negative site will polarize the charge density around the σ -hole or π -hole, thereby affecting both the magnitude and the location of the $V_{S,max}$.

Given all this, do the $V_{S,max}$ have any physical significance? Surprisingly, they do. Detailed studies have shown that the locations of the $V_{S,max}$ associated with σ -holes and π -holes are approximately consistent with the directionalities of interactions [2,5]. This is especially true in the gas phase, but often in the crystal as well, despite the proximities of other molecules increasing the likelihood of secondary effects.

Perhaps even more surprising are the good correlations that have repeatedly been found between the $V_{S,max}$ of a series of σ -hole molecules and their interaction energies ΔE with a given negative site [3,11,68–71]. The interactions become stronger as the $V_{S,max}$ are more positive. For two series of Group IV–VII σ -hole molecules interacting with NH_3 and with HCN , the R^2 values were 0.95 and 0.98, respectively [3].

If different negative sites are involved, then their most negative potentials ($V_{S,min}$) must also be taken into account via a double regression analysis:

$$\Delta E = aV_{S,max} + bV_{S,min} + c \quad (2)$$

For 20 Group IV–VII σ -hole molecules interacting with NH_3 and with HCN , the ΔE predicted by Equation (2) plotted against those computed directly produced an R^2 of 0.94 [3]. Particularly notable is a double regression analysis for 39 complexes involving Groups IV–VII plus hydrogen and six different negative sites [71]. The predicted vs. computed ΔE had $R^2 = 0.91$, despite the varied nature of the database.

The magnitudes and locations of the $V_{S,max}$ clearly do have some physical significance, but caution is always warranted. Sometimes polarization does need to be taken explicitly into account to explain interaction energies [2,3,72–75]. This seems to be especially true when π -holes are involved [2,3,73], although there is again a tendency for interactions to become stronger as $V_{S,max}$ is more positive. The situation for complexes resulting from π -holes merits further study.

5. Overlapping of Positive Potentials: Implications for Interpretation of Close Contacts

It is customary to establish the presence of noncovalent interactions, e.g., in crystals, by looking for “close contacts”. By this is meant interatomic distances that are less than the sum of the van der Waals radii of the respective atoms. One problem with this criterion is the uncertainty associated with the commonly used van der Waals radii, which has been pointed out on several occasions [8,76–78]; this is likely to cause some noncovalent interactions to be overlooked.

A second problem is that the interactions are in reality between the most positive and negative sites, and these do not necessarily coincide with atoms. Consider the heterocycle **1**. It would be anticipated that the selenium will have two σ -holes on the extensions of the C–Se bonds, with resulting positive electrostatic potentials and $V_{S,max}$. Each carbon would similarly be expected to have two σ -holes because of the electron-withdrawing fluorines. What is found instead is a total of only four $V_{S,max}$ and these are not associated with any of the ring atoms but rather are at intermediate locations between the ring atoms; see Figure 4a,b. Evidently, the positive potentials due to the σ -holes on the extensions of the ring bonds overlap, resulting in just one $V_{S,max}$ for each pair of neighboring ring atoms. That $V_{S,max}$ is located between the two atoms.

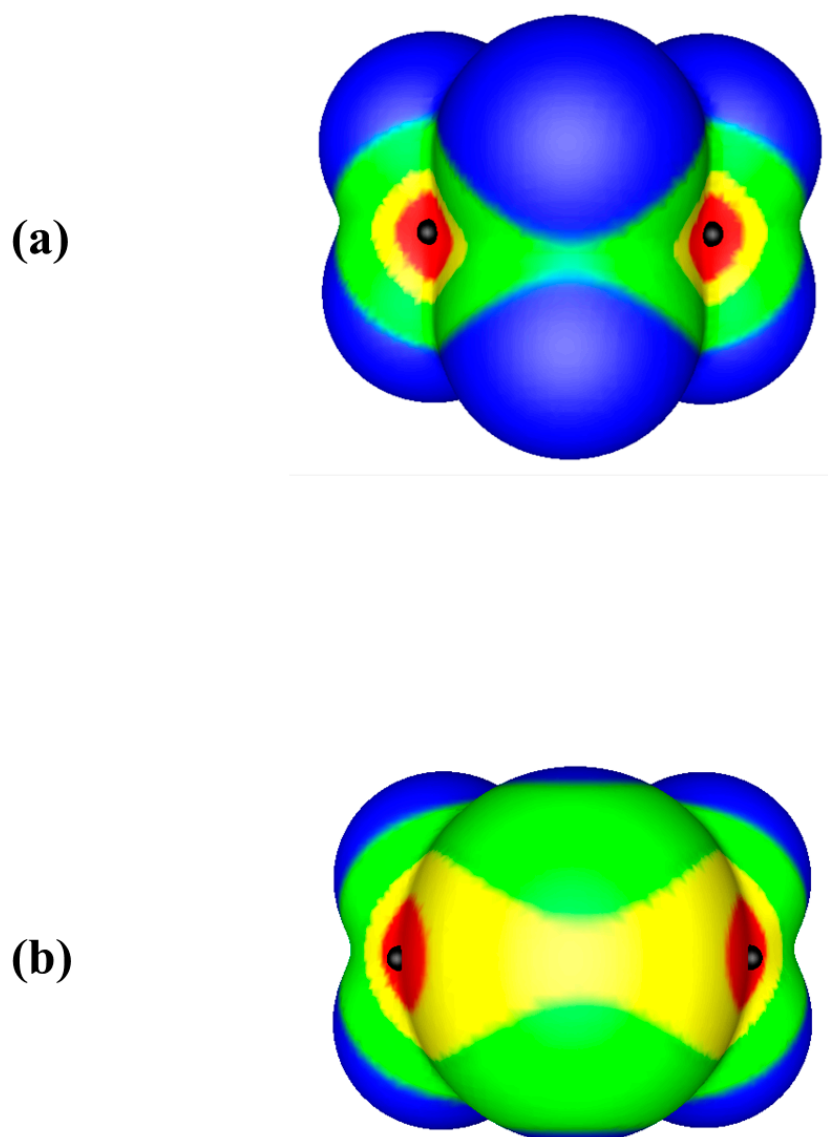
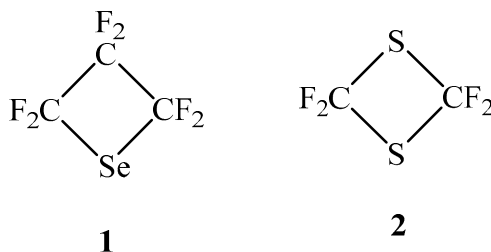


Figure 4. Computed electrostatic potential on 0.001 au molecular surface of the heterocycle **1**. (a) One CF_2 group is in the center foreground, the other two are in the left rear and right rear. Black hemispheres indicate $V_{S,\text{max}}$ near centers of C–C bonds. (b) The selenium is in the foreground, two CF_2 groups are visible at left rear and right rear. Black hemispheres correspond to $V_{S,\text{max}}$ near centers of Se–C bonds. Color ranges, in kcal/mol: red, more positive than 20; yellow, between 20 and 10, green, between 10 and 0; blue, negative.



Do the locations of the $V_{S,\text{max}}$ actually indicate where interactions with negative sites will occur? To test this, we have allowed HCN to interact with **1** through the nitrogen lone pair. Two stable products were obtained, using the M06-2X/6-31+G(d,p) procedure. In one, the nitrogen is positioned near the center of a C–C bond (Figure 5a); in the other, the nitrogen is near the center of a Se–C bond

(Figure 5b). (The HCN is slightly tilted in the latter, likely due to a secondary attraction of its positive C–H portion and the nearby fluorines.)

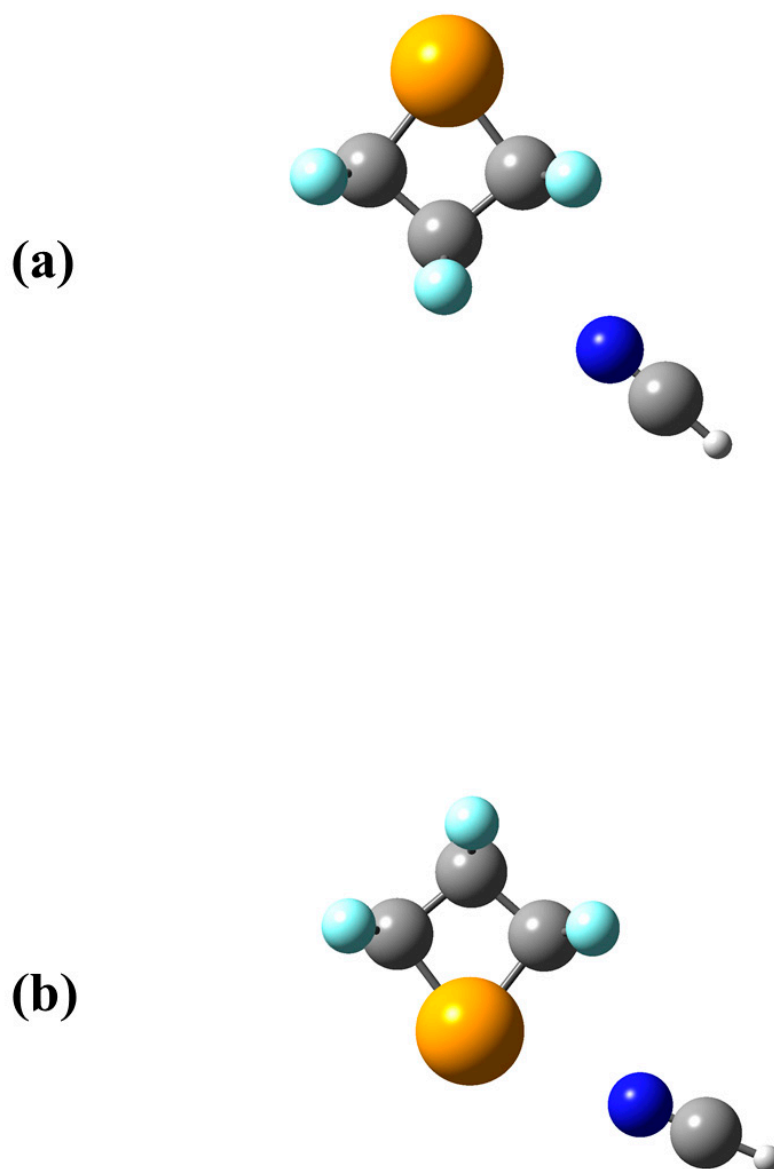


Figure 5. Computed structures of products of interactions between heterocycle **1** and HCN. Colors of atoms: gray, carbon; light blue, fluorine; white, hydrogen; blue, nitrogen; gold, selenium. (a) The nitrogen is positioned near the center of a C–C bond; in the other, (b) The nitrogen is near the center of a Se–C bond.

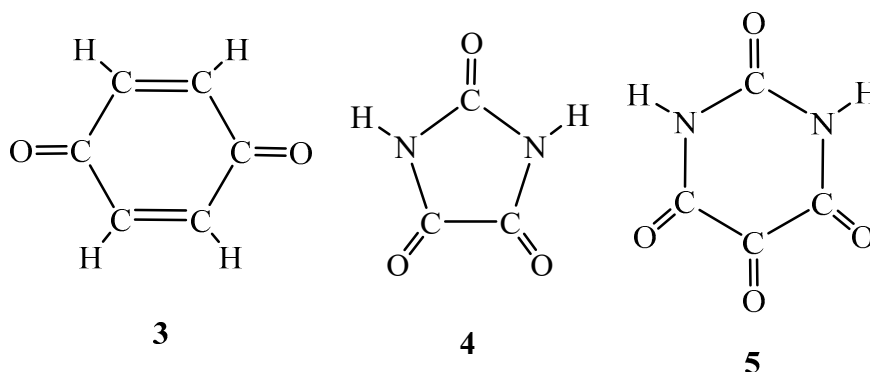
In both cases, the interaction site corresponds to the location of a $V_{S,max}$ near the center of a ring bond, even though the nitrogen can also be described as being in “close contact” with both of the atoms forming that bond. In Figure 5a, the N–C distances are 3.06 Å and 3.09 Å, both less than the sum of Bondi’s nitrogen and carbon van der Waals radii, 3.25 Å [76]. In Figure 5b, the nitrogen is 2.99 Å from the selenium and 3.14 Å from the carbon, while the sums of the respective van der Waals radii are 3.45 Å and 3.25 Å. There are indeed close contacts, but they do not reveal the actual sites of the interactions.

An analogous situation was found crystallographically involving the dithietane, **2**. Again, the heterocyclic ring has just four $V_{S,max}$, located near the centers of the S–C bonds [79]. The structure of the crystal lattice shows that the intermolecular interactions are between a fluorine on one molecule

and one of these $V_{S,max}$ on another, even though the F—C and F—S separations are all less than the sums of the atoms' van der Waals radii.

Are these interactions in the crystal lattice of 2 chalcogen bonds or tetrel bonds? They do pose a problem for that classification scheme. Similar questions arise for 1 and for other heterocyclic systems [5,33,34,80].

Moving on to π -hole interactions, particularly interesting are some cyclic polyketone compounds. As a starting point, we look at 1,4-benzoquinone, 3. Figure 6 shows that the electrostatic potential is positive above and below the ring, with separate $V_{S,max}$ of 17 kcal/mol above and below each carbonyl carbon, corresponding to π -holes.



For contrast, consider parabanic acid (4) and alloxan (5). These are planar molecules, with remarkably high crystal densities, 1.721 g/cm³ [81] and 1.93 g/cm³ [82,83], respectively. (To put these values in perspective, a survey of oxohydrocarbons in the Cambridge Structural Database found that the great majority of them have crystal densities less than 1.40 g/cm³ [84]).

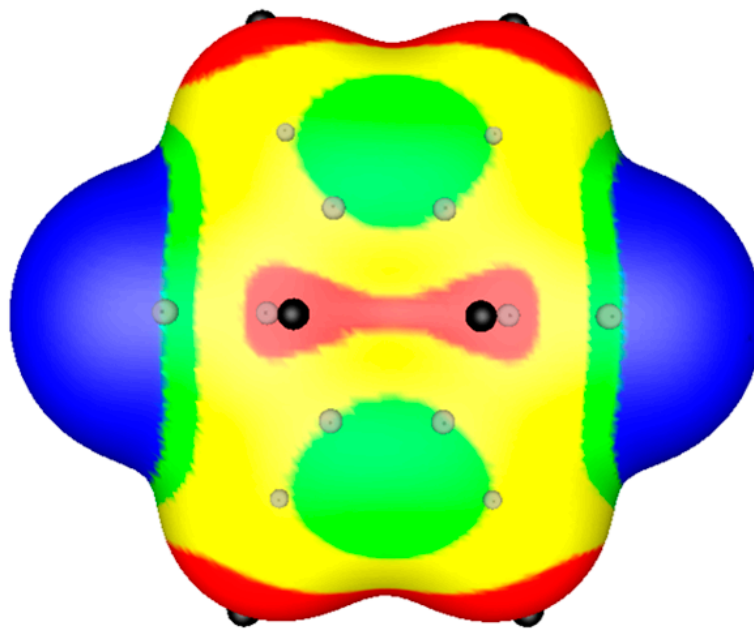


Figure 6. Computed electrostatic potential on 0.001 au molecular surface of 1,4-benzoquinone, 3, which is planar. The oxygens are at the left and right. Gray circles indicate positions of nuclei. Black hemispheres correspond to $V_{S,max}$ due to π -holes above and below carbonyl carbons and σ -holes on hydrogens on extensions of C—H bonds. Color ranges, in kcal/mol: red, more positive than 14; yellow, between 14 and 7; green, between 7 and 0; blue, negative.

In Figure 7 is the electrostatic potential on the 0.001 au surface of parabanic acid, 4. It is again positive above and below the ring, but unlike 3 (Figure 6), there are no $V_{S,max}$ above and below the

carbonyl carbons. In **4**, overlapping of the strongly positive regions due to the π -holes of the carbonyl carbons results in a single $V_{S,max}$ of 33 kcal/mol above and below the approximate center of the ring. The situation in alloxan, **5**, is exactly analogous; an earlier study showed that there are single $V_{S,max}$ above and below the central portion of the ring [33].

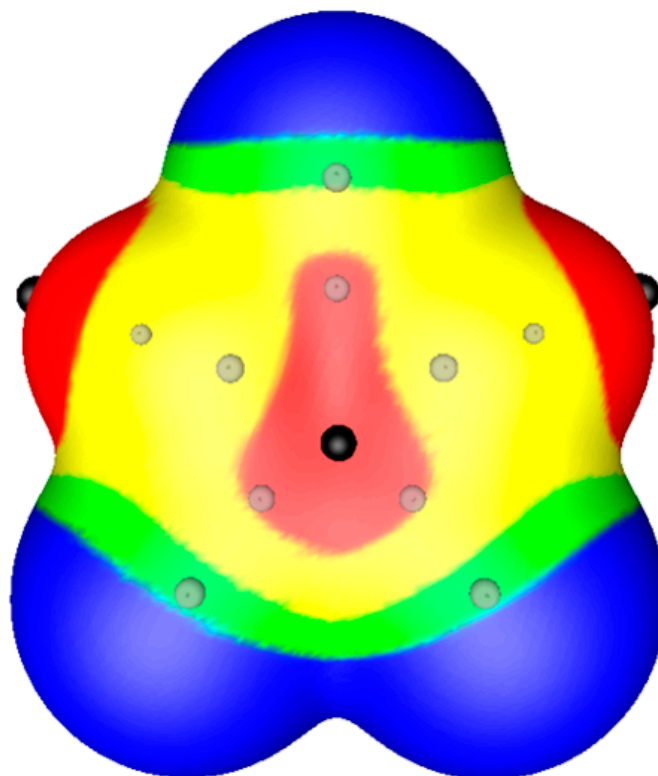


Figure 7. Computed electrostatic potential on 0.001 au molecular surface of parabanic acid, **4**, which is planar. The oxygens are at top and bottom left and right. Gray circles indicate positions of nuclei. Black hemispheres correspond to $V_{S,max}$ due to π -holes above and below approximate center of ring and σ -holes on hydrogens on extensions of C–H bonds. Color ranges, in kcal/mol: red, more positive than 24; yellow, between 24 and 12; green, between 12 and 0; blue, negative.

A particularly intriguing feature of parabanic acid, **4**, and alloxan, **5** (as well as some other cyclic polyketones), was pointed out by Bent in 1968 [14] and later by others [85–87]. The crystal structures of **4** and **5** show that the dominant intermolecular interactions in their crystal lattices are not, as might be expected, between the acidic N–H hydrogens and carbonyl oxygens. Instead, they involve a carbonyl group on one molecule interacting through its oxygen with an adjacent molecule in a roughly perpendicular manner.

Figure 7 and the electrostatic potential of alloxan [33] suggest that the dominant intermolecular interactions in the crystal lattices of **4** and **5** are not between carbonyl oxygens and carbonyl carbons of neighboring molecules, as has been suggested [14,85–87], even though these fit the definition of close contacts. It is the interactions between carbonyl oxygens and the strongly positive potentials above and below the approximate centers of neighboring molecules that primarily stabilize the lattices of **4** and **5**.

Why do these interactions dominate over N–H—O hydrogen bonding in **4** and **5**? Figure 7 suggests that one factor may be the greater accessibility of the large positive regions above and below the rings (and consequently less intermolecular O—O repulsion) compared to the smaller positive regions of the hydrogens.

6. Summary

Quantum mechanics, through the Schrödinger equation and the Hellmann–Feynman theorem, shows that noncovalent intermolecular bonding is Coulombic, i.e., electrostatics and polarization, involving localized positive and negative electrostatic potentials on the molecules. The positive potentials are very often due to the regions of lower electronic density known as σ -holes and π -holes, but they do not necessarily coincide with these regions. Thus, the widely used terms “ σ -hole interaction” and “ π -hole interaction” are somewhat misleading. The interactions are not with the σ -holes and π -holes themselves but rather with the positive potentials that may result from them but may be significantly removed from them.

Using interatomic close contacts as criteria for the existence of nonbonding interactions can similarly be misleading. The positive and/or negative electrostatic potentials that are in reality responsible for the interactions may not coincide with any atom positions. In such cases, close contacts, even if present, do not reveal the actual interactions.

For the great majority of noncovalent bonds, the positive potentials can be attributed to the lower electronic densities of σ -holes or π -holes. The important distinction between these two categories is directionality. σ -Holes and the interactions that result from them are approximately along the extensions of the bonds that resulted in the σ -holes (or occasionally between the extensions of these bonds). π -Holes and the resulting interactions are approximately perpendicular to planar portions of the molecules. Apart from this key difference, however, they are all straightforward Coulombic interactions and can be understood in terms of electrostatics and polarization.

The current practice of labeling interactions by the names of their Groups in the Periodic Table, while seemingly logical, obscures the fundamental unifying similarity within each of the categories: σ -hole and π -hole. Furthermore, in using Group labels, it must be understood that this ignores the one significant way in which the interactions may differ: their directionalities. It also leads to ambiguities, e.g., how to label interactions involving positive regions that result from the overlap of those in two different Groups.

We hope that overanalysis of nonbonding interactions associated with σ -holes and π -holes does not subject them to the same fate as befell the venerable hydrogen bond. It has been dissected into classical and nonclassical, proper and improper (immoral?), blue-shifted and red-shifted, dihydrogen, anti-hydrogen (rebellious?), resonance-assisted, polarization-assisted, and more. All this for a straightforward Coulombic interaction [88,89], one that has been demonstrated to originate from σ -holes on the hydrogens [11,21].

Author Contributions: P.P. wrote the original draft and was involved with analysis. J.S.M. did the computing, prepared the graphics and was involved with analysis.

Funding: No funding was involved.

Conflicts of Interest: The authors declare no conflicts of interest.

References

1. Schneider, H.-J. Binding Mechanisms in Supramolecular Complexes. *Angew. Chem. Int. Ed.* **2009**, *48*, 3924–3977. [[CrossRef](#)]
2. Murray, J.S.; Lane, P.; Clark, T.; Riley, K.E.; Politzer, P. σ -Holes, π -Holes and Electrostatically-Driven Interactions. *J. Mol. Model.* **2012**, *18*, 541–548. [[CrossRef](#)]
3. Politzer, P.; Murray, J.S. Halogen Bonding and Other σ -Hole Interactions: A Perspective. *Phys. Chem. Chem. Phys.* **2013**, *15*, 11178–11189. [[CrossRef](#)] [[PubMed](#)]
4. Bauzá, A.; Mooibroek, T.J.; Frontera, A. The Bright Future of Unconventional σ/π -Hole Interactions. *ChemPhysChem* **2015**, *16*, 2496–2517. [[CrossRef](#)] [[PubMed](#)]
5. Politzer, P.; Murray, J.S.; Clark, T.; Resnati, G. The σ -Hole Revisited. *Phys. Chem. Chem. Phys.* **2017**, *19*, 32166–32178. [[CrossRef](#)] [[PubMed](#)]

6. Stevens, E.D. Experimental Electron Density Distributions of Molecular Chlorine. *Mol. Phys.* **1979**, *37*, 27–45. [[CrossRef](#)]
7. Row, T.N.G.; Parthasarathy, R. Directional Preferences of Nonbonded Atomic Contacts with Divalent Sulfur in Terms of Its Orbital Orientations. 2. S—S Interactions and Nonspherical Shape of Sulfur in Crystals. *J. Am. Chem. Soc.* **1981**, *103*, 477–479. [[CrossRef](#)]
8. Nyburg, S.C.; Faerman, C.H. A Revision of Van der Waals Atomic Radii for Molecular Crystals: N, O, F, S, Cl, Se, Br and I Bonded to Carbon. *Acta Cryst.* **1985**, *B41*, 274–279. [[CrossRef](#)]
9. Ikuta, S. Anisotropy of Electron Density Distribution Around Atoms in Molecules: N, P, O and S Atoms. *J. Mol. Struct. (Theochem)* **1990**, *205*, 191–201. [[CrossRef](#)]
10. Tsirelson, V.C.; Zou, P.F.; Tang, T.-H.; Bader, R.F.W. Topological Definition of Crystal Structure Determination of the Bonded Interactions in Solid Molecular Chlorine. *Acta Cryst.* **1995**, *A51*, 143–153. [[CrossRef](#)]
11. Politzer, P.; Murray, J.S. Halogen Bonding: An Interim Discussion. *ChemPhysChem* **2013**, *14*, 278–294. [[CrossRef](#)] [[PubMed](#)]
12. Benesi, H.A.; Hildebrand, J.H. A Spectrophotometric Investigation of the Interaction of Iodine with Aromatic Hydrocarbons. *J. Am. Chem. Soc.* **1949**, *71*, 2703–2707. [[CrossRef](#)]
13. Hassel, O.; Rømming, C. Direct Structural Evidence for Weak Charge Transfer Bonds in Solids Containing Chemically Saturated Molecules. *Quart. Rev. Chem. Soc.* **1962**, *16*, 1–18. [[CrossRef](#)]
14. Bent, H.A. Structural Chemistry of Donor-Acceptor Interactions. *Chem. Rev.* **1968**, *68*, 587–648. [[CrossRef](#)]
15. Blackstock, S.C.; Lorand, J.P.; Kochi, J.K. Charge-Transfer Interactions of Amines with Tetrahalomethanes. X-Ray Crystal Structures of the Donor-Acceptor Complexes of Quinuclidine and Diazabicyclo[2.2.2]octane with Carbon Tetrabromide. *J. Org. Chem.* **1987**, *52*, 1451–1460. [[CrossRef](#)]
16. Ramasubbu, N.; Parthasarathy, R.; Murray-Rust, P. Angular Preferences of Intermolecular Forces Around Halogen Centers: Preferred Directions of Approach of Electrophiles and Nucleophiles Around Carbon-Halogen Bond. *J. Am. Chem. Soc.* **1986**, *108*, 4308–4314. [[CrossRef](#)]
17. Rosenfeld, R.E., Jr.; Parthasarathy, R.; Dunitz, J.D. Directional Preferences of Nonbonded Atomic Contacts with Divalent Sulfur. 1. Electrophiles and Nucleophiles. *J. Am. Chem. Soc.* **1977**, *99*, 4860–4862. [[CrossRef](#)]
18. Politzer, P.; Murray, J.S.; Janjič, G.V.; Zarič, S.D. σ -Hole Interactions of Covalently-Bonded Nitrogen, Phosphorus and Arsenic: A Survey of Crystal Structures. *Crystals* **2014**, *4*, 12–31. [[CrossRef](#)]
19. Mishra, P.K.; Ekielski, A. The Self-Assembly of Lignin and Its Application in Nanoparticle Synthesis: A Short Review. *Nanomaterials* **2019**, *9*, 243. [[CrossRef](#)]
20. Scilabra, P.; Terraneo, G.; Resnati, G. The Chalcogen Bond in Crystalline Solids: A World Parallel to Halogen Bond. *Acc. Chem. Res.* **2019**, in press.
21. Shields, Z.; Murray, J.S.; Politzer, P. Directional Tendencies of Halogen and Hydrogen Bonding. *Int. J. Quantum Chem.* **2010**, *110*, 2823–2832. [[CrossRef](#)]
22. Metrangolo, P.; Neukirch, H.; Pilati, T.; Resnati, G. Halogen Bonding Based Recognition Processes: A World Parallel to Hydrogen Bonding. *Acc. Chem. Res.* **2005**, *38*, 386–395. [[CrossRef](#)] [[PubMed](#)]
23. Cavallo, G.; Metrangolo, P.; Pilati, T.; Resnati, G.; Terraneo, G. Naming Interactions from the Electrophilic Site. *Cryst. Growth Des.* **2014**, *14*, 2697–2702. [[CrossRef](#)]
24. Stewart, R.F. On the Mapping of Electrostatic Properties from Bragg Diffraction Data. *Chem. Phys. Lett.* **1979**, *65*, 335–342. [[CrossRef](#)]
25. Politzer, P.; Truhlar, D.G. *Chemical Applications of Atomic and Molecular Electrostatic Potentials*; Plenum Press: New York, NY, USA, 1981.
26. Klein, C.L.; Stevens, E.D. Charge Density Studies of Drug Molecules. In *Structure and Reactivity*; Liebman, J.F., Goldberg, A., Eds.; VCH Publishers: New York, NY, USA, 1988; pp. 26–64.
27. Price, S.L. Applications of Realistic Modelling to Molecules in Complexes, Solids and Proteins. *J. Chem. Soc. Faraday Trans.* **1996**, *92*, 2997–3008. [[CrossRef](#)]
28. Murray, J.S.; Politzer, P. The Electrostatic Potential: An Overview. *WIREs Comput. Mol. Sci.* **2011**, *1*, 153–163. [[CrossRef](#)]
29. Bader, R.F.W.; Carroll, M.T.; Cheeseman, J.R.; Chang, C. Properties of Atoms in Molecules. Atomic Volumes. *J. Am. Chem. Soc.* **1987**, *109*, 7968–7979. [[CrossRef](#)]
30. Politzer, P.; Murray, J.S. Molecular Electrostatic Potentials and Chemical Reactivity. In *Reviews in Computational Chemistry*; Lipkowitz, K.B., Boyd, D.B., Eds.; VCH Publishers: New York, NY, USA, 1991; Volume 2, pp. 273–312.

31. Wheeler, S.E.; Houk, K.N. Through-Space Effects of Substituents Dominate Molecular Electrostatic Potentials of Substituted Arenes. *J. Chem. Theory Comput.* **2009**, *5*, 2301–2312. [[CrossRef](#)]
32. Murray, J.S.; Politzer, P. Molecular Electrostatic Potentials and Noncovalent Interactions. *WIREs Comput. Mol. Sci.* **2017**, *7*, e1326. [[CrossRef](#)]
33. Politzer, P.; Murray, J.S. σ -Holes and π -Holes: Similarities and Differences. *J. Comput. Chem.* **2017**, *39*, 464–471. [[CrossRef](#)]
34. Politzer, P.; Murray, J.S. σ -Hole Interactions: Perspectives and Misconceptions. *Crystals* **2017**, *7*, 212. [[CrossRef](#)]
35. Bader, R.F.W.; Henneker, W.H.; Cade, P.E. Molecular Charge Distributions and Chemical Binding. *J. Chem. Phys.* **1967**, *46*, 3341–3363. [[CrossRef](#)]
36. Frisch, M.J.; Trucks, G.W.; Schlegel, H.B.; Scuseria, G.E.; Robb, M.A.; Cheeseman, J.; Scalmani, G.; Barone, V.; Mennucci, B.; Petersson, G. *Gaussian 09, Revision A.1*; Gaussian, Inc.: Wallingford, CT, USA, 2009.
37. Bulat, F.A.; Toro-Labbé, A.; Brinck, T.; Murray, J.S.; Politzer, P. Quantitative Analysis of Molecular Surfaces: Volumes, Electrostatic Potentials and Average Local Ionization Energies. *J. Mol. Model.* **2010**, *16*, 1679–1691. [[CrossRef](#)]
38. Hellmann, H. *Einführung in die Quantenchemie*; Deuticke: Leipzig, Germany, 1937.
39. Feynman, R.P. Forces in Molecules. *Phys. Rev.* **1939**, *56*, 340–343. [[CrossRef](#)]
40. Reed, A.E.; Curtiss, L.A.; Weinhold, F. Intermolecular Interactions from a Natural Bond Orbital, Donor-Acceptor Viewpoint. *Chem. Rev.* **1988**, *88*, 899–926. [[CrossRef](#)]
41. Bader, R.F.W. Pauli Repulsions Exist Only in the Eye of the Beholder. *Chem. Eur. J.* **2006**, *12*, 2896–2901. [[CrossRef](#)]
42. Lennard-Jones, J.E.; Pople, J.A. The Molecular Orbital Theory of Chemical Valency: IX. The Interaction of Paired Electrons in Chemical Bonds. *Proc. R. Soc. Lond. Ser. A* **1951**, *210*, 190–206.
43. Politzer, P.; Riley, K.E.; Bulat, F.A.; Murray, J.S. Perspectives on Halogen Bonding and Other σ -Hole Interactions: Lex parsimoniae (Occam's Razor). *Comput. Theoret. Chem.* **2012**, *998*, 2–8. [[CrossRef](#)]
44. Politzer, P.; Murray, J.S.; Clark, T. σ -Hole Bonding: A Physical Interpretation. *Top. Curr. Chem.* **2015**, *358*, 19–42.
45. Politzer, P.; Murray, J.S.; Clark, T. Mathematical Modeling and Physical Reality in Noncovalent Interactions. *J. Mol. Model.* **2015**, *21*, 52. [[CrossRef](#)]
46. Levine, I.N. *Quantum Chemistry*, 5th ed.; Prentice-Hall: Upper Saddle River, NJ, USA, 2000.
47. Solimannejad, M.; Malekani, M.; Alkorta, I. Cooperative and Diminutive Unusual Weak Bonding in $F_3C-X-HMgH-Y$ and $F_3C-X-Y-HMgH$ Trimers ($X = Cl, Br$; $Y = HCN$ and HNC). *J. Phys. Chem. A* **2010**, *114*, 12106–12111. [[CrossRef](#)]
48. Hennemann, M.; Murray, J.S.; Politzer, P.; Riley, K.E.; Clark, T. Polarization-Induced σ -Holes and Hydrogen Bonding. *J. Mol. Model.* **2012**, *18*, 2461–2469. [[CrossRef](#)]
49. Clark, T.; Politzer, P.; Murray, J.S. Correct Electrostatic Treatment of Non-Covalent Interactions: The Importance of Polarisation. *WIREs Comput. Mol. Sci.* **2015**, *5*, 169–177. [[CrossRef](#)]
50. Riley, K.E.; Hobza, P. Investigations into the Nature of Halogen Bonding Including Symmetry Adapted Perturbation Theory Analyses. *J. Chem. Theory Comput.* **2008**, *4*, 232–242. [[CrossRef](#)]
51. Mulliken, R.S. Molecular Compounds and Their Spectra. II. *J. Am. Chem. Soc.* **1952**, *74*, 811–824. [[CrossRef](#)]
52. Flurry, R.L., Jr. Molecular Orbital Theory of Electron Donor-Acceptor Complexes. I. A Simple Semiempirical Treatment. *J. Phys. Chem.* **1969**, *69*, 1927–1933. [[CrossRef](#)]
53. Dewar, M.J.S.; Thompson, C.C. A Critique for Charge Transfer and Stability Constants for Some TCNE-Hydrocarbon Complexes. *Tetrahedron* **1966**, *7*, 97–114. [[CrossRef](#)]
54. Slifkin, M.A. *Charge Transfer Interactions of Biomolecules*; Academic Press: London, UK, 1971.
55. Stone, A.J.; Price, S.L. Some New Ideas in the Theory of Intermolecular Forces: Anisotropic Atom-Atom Potentials. *J. Phys. Chem.* **1988**, *92*, 3325–3335. [[CrossRef](#)]
56. Sokalski, W.A.; Roszak, S.M. Efficient Techniques for the Decomposition of Intermolecular Interaction Energy at SCF Level and Beyond. *J. Mol. Struct. (Theochem)* **1991**, *234*, 387–400. [[CrossRef](#)]
57. Stone, A.J.; Misquitta, A.J. Charge-Transfer in Symmetry-Adapted Perturbation Theory. *Chem. Phys. Lett.* **2009**, *473*, 201–205. [[CrossRef](#)]
58. Stone, A.J. Natural Bond Orbitals and the Nature of the Hydrogen Bond. *J. Phys. Chem. A* **2017**, *121*, 1531–1534. [[CrossRef](#)]

59. Clark, T.; Murray, J.S.; Politzer, P. A Perspective on Quantum Mechanics and Chemical Concepts in Describing Noncovalent Interactions. *Phys. Chem. Chem. Phys.* **2018**, *20*, 30076–30082. [[CrossRef](#)] [[PubMed](#)]
60. Brinck, T.; Borrfors, A.N. Electrostatics and Polarization Determine the Strength of the Halogen Bond: A Red Card for Charge Transfer. *J. Mol. Model.* **2019**, in press.
61. Wang, W.; Wang, N.B.; Zheng, W.; Tian, A. Theoretical Study on the Blueshifting Halogen Bond. *J. Phys. Chem. A* **2004**, *108*, 1799–1805. [[CrossRef](#)]
62. Murray, J.S.; Concha, M.C.; Lane, P.; Hobza, P.; Politzer, P. Blue Shifts vs. Red Shifts in σ -Hole Bonding. *J. Mol. Model.* **2008**, *14*, 699–704. [[CrossRef](#)] [[PubMed](#)]
63. Ramasubbu, N.; Parthasarathy, R. Stereochemistry of Incipient Electrophilic and Nucleophilic Reactions at Divalent Selenium Center: Electrophilic-Nucleophilic Pairing and Anisotropic Shape of Se in Se . . . Se Interactions. *Phosphorus Sulfur* **1987**, *31*, 221–229. [[CrossRef](#)]
64. Politzer, P.; Murray, J.S.; Concha, M.C. Halogen Bonding and the Design of New Materials: Organic Bromides, Chlorides and Perhaps Even Fluorides as Donors. *J. Mol. Model.* **2007**, *13*, 643–650. [[CrossRef](#)]
65. Chopra, D.; Guru Row, T.N. Role of Organic Fluorine in Crystal Engineering. *CrystEngComm* **2011**, *13*, 2175–2186. [[CrossRef](#)]
66. Metrangolo, P.; Murray, J.S.; Pilati, T.; Politzer, P.; Resnati, G.; Terraneo, G. Fluorine-Centered Halogen Bonding: A Factor in Recognition Phenomena and Reactivity. *Cryst. Growth Des.* **2011**, *11*, 4238–4246. [[CrossRef](#)]
67. Pathak, R.K.; Gadre, S.R. Maximal and Minimal Characteristics of Molecular Electrostatic Potentials. *J. Chem. Phys.* **1990**, *93*, 1770–1773. [[CrossRef](#)]
68. Riley, K.E.; Murray, J.S.; Politzer, P.; Concha, M.C.; Hobza, P. Br—O Complexes as Probes of Factors Affecting Halogen Bonding: Interactions of Bromobenzenes and Bromopyrimidines with Acetone. *J. Chem. Theory Comput.* **2009**, *5*, 155–163. [[CrossRef](#)] [[PubMed](#)]
69. Riley, K.E.; Murray, J.S.; Fanfrlík, J.; Řezáč, J.; Solá, R.J.; Concha, M.C.; Ramos, F.M.; Politzer, P. Halogen Bond Tunability I: The Effects of Aromatic Fluorine Substitution on the Strengths of Halogen-Bonding Interactions Involving Chlorine, Bromine and Iodine. *J. Mol. Model.* **2011**, *17*, 3309–3318. [[CrossRef](#)]
70. Bundhun, A.; Ramasami, P.; Murray, J.S.; Politzer, P. Trends in σ -Hole Strengths and Interactions of F_3MX Molecules ($M = C, Si, Ge$ and $X = F, Cl, Br, I$). *J. Mol. Model.* **2013**, *19*, 2739–2746. [[CrossRef](#)]
71. Politzer, P.; Murray, J.S. A Unified View of Halogen Bonding, Hydrogen Bonding and Other σ -Hole Interactions. In *Noncovalent Forces*; Scheiner, S., Ed.; Springer: Heidelberg, Germany, 2015; Chapter 10; pp. 291–321.
72. Politzer, P.; Murray, J.S. Halogen Bonding and Beyond: Factors Influencing the Nature of CN-R and SiN-R Complexes with FCl and Cl₂. *Theoret. Chem. Acc.* **2012**, *131*, 1114. [[CrossRef](#)]
73. Murray, J.S.; Shields, Z.P.-I.; Seybold, P.G.; Politzer, P. Intuitive and Counterintuitive Noncovalent Interactions of Aromatic π -Regions with the Hydrogen and Nitrogen of HCN. *J. Comput. Sci.* **2015**, *10*, 209–216. [[CrossRef](#)]
74. Clark, T.; Hesselmann, A. The Coulombic σ -Hole Model Describes Bonding in $CX_3I \cdots Y^-$ Complexes Completely. *Phys. Chem. Chem. Phys.* **2018**, *20*, 22849–22855. [[CrossRef](#)] [[PubMed](#)]
75. Clark, T.; Murray, J.S.; Politzer, P. The σ -Hole Coulombic Interpretation of Trihalide Anion Formation. *ChemPhysChem* **2018**, *19*, 3044–3049. [[CrossRef](#)] [[PubMed](#)]
76. Bondi, A. Van der Waals Volumes and Radii. *J. Phys. Chem.* **1964**, *68*, 441–451. [[CrossRef](#)]
77. Dance, I. Distance Criteria for Crystal Packing Analysis of Supramolecular Motifs. *New J. Chem.* **2003**, *27*, 22–27. [[CrossRef](#)]
78. Alvarez, S. A Cartography of the van der Waals Territories. *Dalton Trans.* **2013**, *42*, 8617–8636. [[CrossRef](#)]
79. Nayak, S.K.; Kumar, V.; Murray, J.S.; Politzer, P.; Terraneo, G.; Pilati, T.; Metrangolo, P.; Renati, G. Fluorination Promotes Chalcogen Bonding in Crystalline Solids. *CrystEngComm* **2017**, *19*, 4955–4959. [[CrossRef](#)]
80. Politzer, P.; Resnati, G.; Murray, J.S. Close Contacts and Noncovalent Interactions in Crystals. *Faraday Disc.* **2017**, *203*, 113–130.
81. Davies, D.R.; Blum, J.J. The Crystal Structure of Parabanic Acid. *Acta Cryst.* **1955**, *8*, 129–136. [[CrossRef](#)]
82. Bolton, W. The Crystal Structure of Alloxan. *Acta Cryst.* **1964**, *17*, 147–152. [[CrossRef](#)]
83. Swaminathan, S.; Craven, B.M.; McMullan, R.K. Alloxan—Electrostatic Properties of an Unusual Structure from X-ray and Neutron Diffraction. *Acta Cryst.* **1985**, *B41*, 113–122. [[CrossRef](#)]
84. Gavezzotti, A. Molecular Packing and Other Structural Properties of Crystalline Oxohydrocarbons. *J. Phys. Chem.* **1991**, *95*, 8948–8955. [[CrossRef](#)]

85. Spackman, M.A.; Weber, H.P.; Craven, B.M. Energies of Molecular Interactions from Bragg Diffraction Data. *J. Am. Chem. Soc.* **1988**, *110*, 775–782. [[CrossRef](#)]
86. Coombes, D.S.; Nagi, G.K.; Price, S.L. On the Lack of Hydrogen Bonds in the Crystal Structure of Alloxan. *Chem. Phys. Lett.* **1997**, *265*, 532–537. [[CrossRef](#)]
87. Paulini, R.; Müller, K.; Diederich, F. Orthogonal Multipolar Interactions in Structural Chemistry and Biology. *Angew. Chem. Int. Ed.* **2005**, *44*, 1788–1805. [[CrossRef](#)]
88. Hunter, C.A. Quantifying Intermolecular Interactions: Guidelines for the Molecular Recognition Toolbox. *Angew. Chem. Int. Ed.* **2004**, *43*, 5310–5324. [[CrossRef](#)]
89. Aakeröy, C.B.; Wijethunga, T.K.; Desper, J. Molecular Electrostatic Potential Dependent Selectivity of Hydrogen Bonding. *New J. Chem.* **2015**, *39*, 822–828. [[CrossRef](#)]



© 2019 by the authors. Licensee MDPI, Basel, Switzerland. This article is an open access article distributed under the terms and conditions of the Creative Commons Attribution (CC BY) license (<http://creativecommons.org/licenses/by/4.0/>).